

Use of a flood-routing model to assess lateral flows in a karstic stream: implications to the hydrogeological functioning of the Grands Causses area (Tarn River, Southern France)

Jean-Baptiste Charlier¹ · Roger Moussa² · Vincent Bailly-Comte¹ · Laurent Danneville³ · Jean-François Desprats² · Bernard Ladouche² · Arthur Marchandise⁴

Received: 20 January 2015 / Accepted: 20 June 2015 / Published online: 4 July 2015
© Springer-Verlag Berlin Heidelberg 2015

Abstract The aim of this study is to assess the spatio-temporal variability of lateral flows in the streams of a large karstic basin to construct a conceptual model of karst contributions to flood generation. The lateral flows of the Tarn River, which crosses the Grands Causses karst zone in Southern France, were investigated between several gauging stations along the river. First, through analysing the lateral flows on an event time scale of 30 floods, it was possible to identify the losing and gaining reaches, highlighting a highly variable attenuation/amplification role of karsts on flood generation. Second, the diffusive wave model was used to quantify the lateral flows on an hourly time step within a flood event. The simulations show a high variability of lateral outflows and inflows within a same reach according to the hydrometeorological conditions, with in some cases an inversion of the lateral flow direction during the flood. The results highlight complex surface/groundwater exchanges during a single flood event, with high river losses despite the concurrent flow of large springs feeding the stream. This spatio-temporal variability of the karst influence on flood generation was linked to the

aquifer's structure, which has improved the understanding of the hydro(geo)logical functioning of the Grands Causses massif. Finally, the new methodology proposed here opens challenging perspectives towards a framework for the analysis of surface–groundwater exchanges in karstic rivers.

Keywords Flood routing · Karst · Lateral flows · Hydrological processes · Surface/groundwater interactions · Diffuse wave model

Introduction

Karst aquifers are recognised as contributing to flood generation in carbonate catchments, notably in a Mediterranean climate where extreme rainfall can generate catastrophic flash floods (Mijatovic 1988; Bonacci et al. 2006; Maréchal et al. 2008; De Waele et al. 2010; Zanon et al. 2010; Kourgialas et al. 2012; Fleury et al. 2013). Understanding their influence on flood generation nevertheless remains a major challenge owing to the complexity of lateral flows, including surface/groundwater interactions, in such a heterogeneous context. Recent studies have enabled an identification of the contribution of karsts and their impact (attenuation or amplification) on peakflow. Stream flows can re-infiltrate karst aquifers (totally in some cases) depending on the aquifer's storage capacity (Bailly-Comte et al. 2009; De Waele et al. 2010; Jourde et al. 2013) and so attenuate the flood peak. Flooding in karst areas can have two origins that can be schematically conceptualised by (1) infiltration excess runoff due to a small retention capacity of the karst medium (Maréchal et al. 2008; Fleury et al. 2013), and (2) backflooding following rapid infiltration with a simultaneous rapid rise of the aquifer's

✉ Jean-Baptiste Charlier
j.charlier@brgm.fr

¹ BRGM, 1039 rue de Pinville, 34000 Montpellier, France

² INRA, UMR LISAH «Laboratoire d'étude des Interactions entre Sol-Agrosystème-Hydrosystème», 2 Place Pierre Viala, 34060 Montpellier Cedex 1, France

³ PNRGC «Parc Naturel Régional des Grands Causses», 71 boulevard de l'Ayrolle, BP 50126, 12101 Millau cedex, France

⁴ SCHAPI «Service Central d'Hydrométéorologie et d'Appui à la Prévision des Inondations», 42 avenue Gaspard Coriolis, 31057 Toulouse Cedex 1, France

water level due to a limited saturation capacity of the conduit network (Lopez-Chicano et al. 2002; Bonacci et al. 2006; Jourde et al. 2007; Bailly-Comte et al. 2008a, b). As an indication of the karst role in flood amplification at catchment scale, contributions controlled by karst saturation can generate event runoff coefficient close to 1 (Maréchal et al. 2008). Knowing that a karst's impact on flood generation can be highly contrasted, identifying its flood attenuation/amplification role is of major interest.

Few studies have investigated lateral flows in karstic basins, mainly because of the scarcity of data and/or the global representation of local measurements in highly heterogeneous media. One interesting approach in this respect is the Inflow–Outflow analysis at catchment scale, which is based on investigating lateral flows between two gauging stations in channel reaches. Applying this approach to the Coulazou River, which crosses the Causse d'Aumelas karstic terrain in Southern France, Bailly-Comte et al. (2009) showed time-variant surface/groundwater exchanges resulting in alternate losses and gains within the reach. The limited discharge capacity of conduits embedded in a low-permeability matrix is considered as a main driver of these exchanges, in conjunction with the aquifer saturation level prior to flooding. Subdividing a river into reaches at each available gauging station and applying the Inflow–Outflow analysis to each reach actually appears to be an efficient approach for assessing the spatial variability of karst influence in larger catchments. It nevertheless requires a flood-routing model to assess the dynamic of the lateral inflows and outflows during a flood event. And in this topic, less physically based flood-routing models accounting for lateral flows were used in karstic basins.

A first approach to account for concentrated lateral flows used the kinematic wave model coupled with a linear underground reservoir (Bailly-Comte et al. 2012). River reaches with many imprecisely localised inflows and outflows, however, also require a model to account for the diffusivity. One such model is the diffusive wave (DW) model, which is a simplification of the Saint–Venant equation and is able to account for lateral flows (see the review in Cimorelli et al. 2014). The Hayami (1951) DW model, in particular, was proposed by Moussa (1996) to account for uniformly distributed lateral flows; it is an analytical, stable and parsimonious solution that has been successfully used in various contexts (Moussa et al. 2002, 2007; Moussa and Bocquillon 2009). It has, however, never been applied to a basin with strong lateral flows, as is often the case in karstic basins.

Here, the aim of this study is to assess the spatio-temporal variability of stream lateral flows in a large karstic basin to improve the knowledge for a conceptual

hydrogeological model of the massif being drained by the river. The case study is the Tarn River that crosses the Grands Causses karstic zone of Southern France and whose large catchment presents common hydrogeological features with other large karstic basins in the Mediterranean context; i.e. an allogenic recharge from a hard-rock area in the head-water catchment, a simple channel network with few tributaries, and an obvious contribution from karst units through numerous springs. The approach involved two steps: first, an analysis of the highest flood events to assess the losing and gaining reaches related to the hydrological response at the flood event time scale; second, use of the Hayami DW model to characterise the dynamic of the lateral flows during flood events along the river. The result is a new conceptual hydrogeological model of the Grands Causses area that illustrates the variability of the hydrological processes involved in relation to the basin's hydrogeological structure.

Study site

Site

Basin presentation

The study site is the Tarn River at Millau in Southern France, which extends from the Cévennes mountains to the Grands Causses karstic region (Fig. 1). The topographic basin covers an area of about 2100 km² with the hydrogeological basin, notably in the karstic zone, being slightly larger with an area of about 2400 km². The Tarn River has two main tributaries: the Dourbie River and the Jonte River. The head-water catchments for these three main streams are located in the western part of the Cévennes mountains with Mont Aigual at 1567 m a.s.l. and Mont Lozère at 1699 m a.s.l. In their intermediate and downstream parts, the three rivers form canyons across the Grands Causses plateaux (between 1100 and 700 m a.s.l.) heading to the outlet at Millau at 350 m a.s.l.

Climate

The climate in the Cévennes mountains is Mediterranean with a mountainous influence, giving high rainfalls, mainly in autumn, that are usually of high intensity and short duration. Over the Grands Causses region, the Mediterranean–mountainous climate is modified by an oceanic influence with lower rainfall intensities and amounts. There is thus a large spatial variability of mean annual rainfall ranging from 750 mm at the outlet near Millau to 2000 mm in the upstream area of the basin.



Fig. 1 Hydrogeological map of the Tarn basin at Millau showing the two hydro-geomorphological zones: the hard-rock area (*pink-coloured units*) in the Cévennes mountains of the upstream part of

the basin, and the karst area (*blue-coloured units*) in the Grands Causses of the intermediate and downstream parts of the basin

Geology and aquifer units

The geological framework consists mainly of an upstream crystalline hard-rock area in the eastern part of the basin and a downstream karstic sedimentary area in the central and western parts of the basin (Fig. 1). The hard-rock area (pink-coloured units covering 31 % of the basin; Fig. 1) is composed mainly of Proterozoic and Palaeozoic basement of plutonic and metamorphic rocks of the Cévennes mountains, whereas the karstic sedimentary area (blue-coloured units covering 69 % of the basin; Fig. 1) is composed of Jurassic limestone, marly limestone and dolomite of the Grands Causses plateaux. The general

hydrogeological pattern of the Grands Causses area comprises two main karst aquifer units separated by a 250-m-thick sequence of Toarcian marl (Bérard 1987; Ricard and Bakalowicz 1996; Plagnes 1997; PNRGC 2006; Dörfliger 2007). The lower unit, between 50 and 300 m thickness, is developed in Lower Jurassic (Hettangian-Sinemurian) limestone and dolomitic limestone overlying Triassic formations covering the crystalline basement; it is exposed at the crystalline/sedimentary contact in the northern part of the basin. The upper unit, more than 400 m thick, is developed in Middle and Upper Jurassic limestone, marly limestone and dolomite; it constitutes the Grands Causses plateaux and the cliffs of the Dourbie, Jonte and Tarn river

gorges, and is the main groundwater reservoir of the karstic area. All the carbonate formations are globally tabular with a low west-dip direction. The formations are cut by predominantly W–E and N–S faults generating hydrogeological discontinuities that delimit aquifer boundaries and drainage axes. Some authors consider a possible connexion between the upper and lower karst units through fault reactivation locally thinning the impervious marl layer (Bérard 1987; PNRGC 2006).

Hydrological and hydrogeological setting

The geological and geomorphological characteristics of the hard-rock and karstic areas generate a specific hydrological and hydrogeological functioning in each hydro-geomorphological zone.

The head-water catchments in the hard-rock area show a marked topography of narrow valleys, steep hillslopes and a herring-bone-shaped channel network. Surface and shallow subsurface processes would seem to predominate in these small sub-basins (Marchandise 2007; Moussa et al. 2007) with the result that the perennial streams have a low baseflow. The high-intensity rainfall events generate high flow volumes leading to flash floods, some of which can be catastrophic in the Cévennes mountains (Delrieu et al. 2005).

The Grands Causses area shows typical karst landforms (dolines, sinkholes, karren zones, ruiniform reliefs) indicating that the karstification is well developed. Here, the Tarn, Dourbie and Jonte rivers have incised the plateau, developing steep-sided gorges some 400–500 m deep. The channel network at the plateaux's surface is limited to intermittent streams (unconnected to the main rivers) drained by dolines or sinkholes. In the upstream part of the karstic area (just downstream of the hard-rock/karst contact) some of the valleys are dry during low water levels (e.g. the Jonte gorges downstream of Meyrueis). In the intermediate and downstream parts of the karstic area, numerous springs at the bottom of the canyons attest to lateral inflows from the karst system to the rivers. These springs are but the visible part of the karst inflows, because numerous spring outlets are known in the Tarn River bed. The river baseflow increases progressively downstream indicating that the rivers drain the upper karst unit aquifers of the Grands Causses. The first quantifications of the karst contribution to the main stream of the Tarn River indicate high groundwater inflows reaching as much as 50 % of the Tarn flow between the Montbrun and La Muse stations (Bérard 1987), and 75 % of the Dourbie River baseflow at Massebiau during low water levels (Ricard and Bakalowicz 1996).

The hydrogeological functioning of the largest karst systems at the study site are relatively well known from the many previous studies carried out using coupled

hydrodynamic and hydrochemical approaches (Ricard and Bakalowicz 1996; Plagnes 1997; Braneyre et al. 1999; Pinault et al. 2001; PNRGC 2006; Dörfliger 2007). The main springs draining the Grands Causses are the Burle and Beldoire on the Sauveterre plateau, and the Espérelle and Durzon on the Larzac plateau. Their annual mean discharges range between 0.6 and 4.0 m³ s⁻¹, with peakflows during highest floods frequently estimated at several tens of m³ s⁻¹ (up to about 35 m³ s⁻¹ for the Espérelle spring; Charlier et al. 2012).

Data

Spatial data

Topographic and geological maps of the study area were obtained from the “Institut National de l'Information Géographique et Forestière (IGN)” and the “Bureau de Recherches Géologiques et Minières (BRGM)”, respectively. Hydrological features of the channel networks and springs were obtained from digitised BD CARTHAGE® (IGN) and the “Banque nationale d'Accès aux Données sur les Eaux Souterraines (ADES 2012)”, respectively.

The recharge areas of the karst systems were delimited from dye-tracing test data, providing information on existing connections between infiltration points and karst outlets (springs) for each plateau. The dye-tracing results, synthesised in Charlier et al. (2012), were obtained from (1) Ricard and Bakalowicz (1996) and PNRGC (2011) for the Causse du Larzac, (2) Ambert et al. (1994) and PNRGC and Cadier (2010) for the Causse Noir, (3) Bérard (1987) for the Causse Méjean, (4) Bérard (1987), PNRGC (2006), and Dörfliger and Meus (2006) for the Causse de Sauveterre, and (5) Braneyre et al. (1999) for the Causse Rouge.

Temporal data

Precipitation data were obtained from “METEO France” records at 15 weather stations distributed over the basin: Le Massegros, Millau, Cavalerie, St-Pierre-des-Tripiers, Ste-Enimie, St Sauveur Camprieux, Alzon, Gatuzières, La Salle Prunet, Rousses, Valleraugue, Mont Aigoual, Le Bley-mard, Bassurels, and St Martin de Lansuscle.

Streamflow hydrographs were obtained from the “Service de Prévision des Crues (SPC) Garonne-Tarn-Lot” records at six gauging stations: Millau, Montbrun and Cocurès on the Tarn River, Florac on the Tarnon River, Nant on the Dourbie River and Meyrueis on the Jonte River. Data were also obtained from the “Direction Départementale des Territoires de Lozère (DDT48)”, and from the “Direction Régionale de l'Environnement, de l'Aménagement et du Logement (DREAL) de Midi-Pyrénées” for the two gauging stations of the Dourbie River at

Massebiau and the Tarn River at La Muse (Mostuéjols), respectively. Lecollinet (2012) checked that the rating curves are confident for the high flow values.

Karst spring discharges were obtained from the “Parc Naturel Régional des Grands Causses” for seven spring stations: Fontmaure, Beldoire, Rouveyrol, Mas Lafont, Font Liane, Espérelle, and Durzon. Data for two additional spring stations were obtained from BRGM/ONEMA/Réseau DCE: Burle, and Cenarette.

All the hydrological and hydrogeological time series were synchronised on a daily time step over the 1998–2012 period. Hourly data were collected for the selected flood events presented in the next section.

Data processing and modelling

Hydrological analysis

Sub-basin boundaries were defined for all the stations according to the following criteria: (1) in the hard-rock area where the geological formations are considered as relatively impervious, the boundaries are considered equal to those of the topographic sub-catchments; (2) in the karst area where karstified limestone crops out and surface runoff is negligible, the boundaries are defined as those of the karst system recharge areas; and (3) in the karst area where marly layers are exposed, the boundaries are defined as those of the topographic sub-catchments. The result of this basin subdivision is shown in Fig. 1, with three head-basins being identified in the hard-rock area and four sub-basins in the karst area. Figure 2 is a simplified outline of this subdivision and Table 1 gives the main characteristics

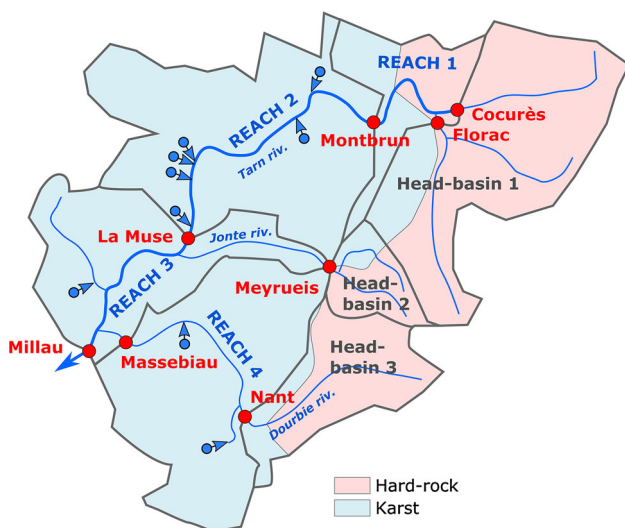


Fig. 2 Diagram of the head-basins and the sub-basins of the four reaches of the Tarn and Dourbie rivers at Millau; the sub-basin characteristics are given in Table 1

of each sub-basin. Four reaches were investigated in the karst area: (1) Reach 1 between Florac + Cocurès and Monbrun, (2) Reach 2 between Monbrun and La Muse, (3) Reach 3 between La Muse + Meyrueis + Massebiau and Millau, and (4) Reach 4 between Nant and Massebiau. Reaches 1, 2 and 3 delimit the upstream, intermediate and downstream karstic zones, respectively, of the Tarn River, whereas Reach 4 characterises the entire karstic zone of the Dourbie tributary. To limit the influence of tributaries when quantifying the lateral flows, each reach inflow was considered as the sum of all the surrounding upstream gauging stations in the hydrographic network. Consequently, unlike Reaches 2 and 4 fed by a single upstream gauging station, Reach 1 is fed by two gauging stations in the hard-rock area, and the Reach 3 is fed by three gauging stations, i.e. one station in the main stream (Tarn River) and two stations on the main tributaries (Jonte and Dourbie rivers).

The storm event selection aims at identifying low- and high-flood events generated by high rainfall under various initial hydric conditions. Firstly, a daily time step selection of the rainfall periods was carried out taking into account the following criteria: a mean daily rainfall intensity in excess of 75 mm over one of the seven sub-catchments. This was followed by an extraction of hourly data during these periods, resulting in the selection of 30 storm events that were then analysed at the hourly time step. Duration of rainfall events ranged between 0.25 and 15 days, with a median value of about 3.4 days. Next the total mean rainfall depth [L] and the maximum rainfall intensity over 1 h [$L T^{-1}$] were estimated for the two hydro-geomorphological zones using a Thiessen polygon interpolation of the rainfall stations. Then, for each reach and its corresponding sub-basin, calculation of the mean rainfall depth was completed by a calculation of the lateral flow depth [L] defined as the ratio between the difference in volume between the Inflows and Outflows [L^3], and the sub-basin area [L^2].

The Hayami diffusive wave model with lateral flows

To assess the contributions of lateral flow between two hydrographic stations at the event time scale, an analytical resolution of the Diffusive Wave (DW) equation with the lateral flow uniformly distributed over a reach (length L) was used with the Hayami assumptions: constant celerity C [$L T^{-1}$] and constant diffusivity D [$L^2 T^{-1}$], and no downstream boundary condition, as proposed by Moussa (1996):

$$O(t) = \Phi(t) + [I(t) - \Phi(t)] * K(t) \quad \text{with}$$

$$\Phi(t) = \frac{C}{L} \int_0^t [Q_A(\lambda) - Q_A(0)] d\lambda \quad (1)$$

where $I(t)$ and $O(t)$ are the upstream (Inflow) and

Table 1 Morphological characteristics of the sub-basins; see Fig. 2 for location of rivers, gauging stations, and sub-basins

Sub-basin	Main river	Inflow gauging station(s)	Outflow gauging station(s)	Surface (km ²)	Rate of Karst outcrop (%)	Reach length (km)	Monitored lateral springs
Head-basin 1	Tarn River	–	Florac + Cocurès	491	13.4	–	–
Head-basin 2	Jonte River	–	Meyrueis	87	19.0	–	–
Head-basin 3	Dourbie River	–	Nant	220	19.8	–	–
Sub-basin of Reach 1	Tarn River	Florac + Cocurès	Montbrun	166	57.6	18	–
Sub-basin of Reach 2	Tarn River	Montbrun	La Muse	590	100.0	44	Burle, Cenarette, Rouveyrol, Beldoire, Fontmaure, Mas de Lafont
Sub-basin of Reach 3	Tarn River	La Muse + Meyrueis + Massebiau	Millau	341	100.0	47	Font Liane
Sub-basin of Reach 4	Dourbie River	Nant	Massebiau	490	99.7	29	Durzon, Espérelle

downstream (Outflow) storm flows, respectively, t is time [T], and $d\lambda$ is the calculation time step. The symbol $*$ represents the mathematical convolution function, and $K(t)$ is expressed as:

$$K(t) = \frac{L}{2(\pi D)^{1/2}} \frac{\exp\left(\frac{cL}{2D}\left(2 - \frac{L}{c} - \frac{c}{L}\right)\right)}{t^{3/2}} \quad (2)$$

The total lateral hydrograph $Q_A(t)$ on the reach, under the hypothesis of uniformly distributed lateral flow ($q(x,t)$ [L² T⁻¹] being the lateral flow per length unit at the x [L] downstream distance), is expressed as:

$$Q_A(t) = \int_0^L q(x, t) \cdot dx \quad (3)$$

Depending on the hydrological conditions, $q(x,t)$ may be positive or negative, respectively, when lateral inflow or outflow from the channel occurs (Fig. 3). The inverse problem concerns the identification of lateral inflow or outflow between two gauging station on the basis of the observed hydrographs $I(t)$ and $O(t)$ at the two stations. According to Moussa (1996) Eq. 1 gives:

$$\Phi(t) - \Phi(t) * K(t) = O(t) - I(t) * K(t) \quad (4)$$

The resolution of Eq. 4 firstly requires identification of $K(t)$ using Eq. 2, and then the calculation of the function $\Phi(t)$. Finally, the lateral inflow or outflow $Q_A(t)$ can be calculated as follows:

$$Q_A(t) = Q_A(0) + \frac{L}{C} \frac{d\Phi}{dt} \quad (5)$$

The flood-routing parameters C and D are constant at the flood event time scale and, as a first approximation, can be estimated for each flood from the hydrograph's characteristics when $I(t)$ and $O(t)$ are known (Moussa 1996), thus avoiding any calibration procedure. The forward model can then be applied by estimating $O(t)$ from the known $I(t)$, and $Q_A(t)$ from Eq. 1, and the inverse model can be used to assess the lateral flow $Q_A(t)$ (knowing both $I(t)$ and $O(t)$ from Eq. 4) and consequently enabling surface–groundwater exchanges within a flood event to be quantified.

Results

Flood event analysis

Rainfall variability

This section aims at analysing the spatial variability of rainfall between the two hydro-geomorphological areas (hard-rock and karstic) of the study site during the 30 storm events. Figure 4a, b presents boxplots of the total mean rainfall depth (P) and the maximum rainfall intensity over 1 h (P_x), respectively. It shows a high spatial variability between the two zones with rainfall events in the hard-rock area, reaching about 200 mm with intensities of more than 10 mm/h, being globally twice as high as in the karstic area. Comparing the boxplot heights, a higher variability of the rainfall events is also observed in the hard-rock area. Because hard-rock areas are located in the upstream

Fig. 3 Diffusive wave model with uniformly distributed lateral flows (from Moussa 1996)

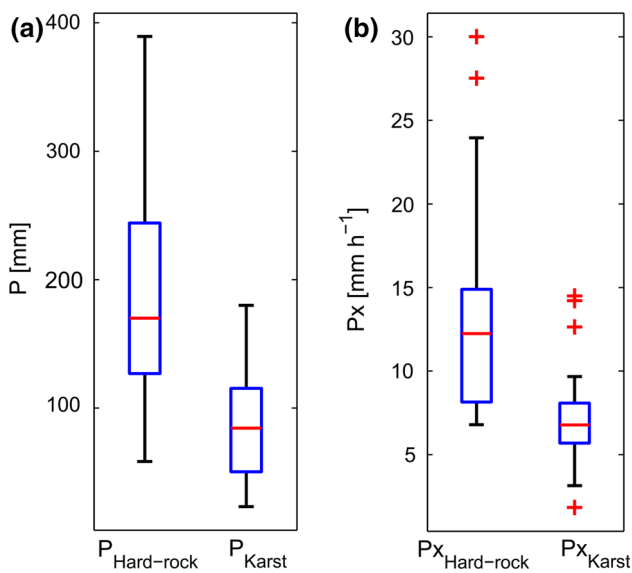
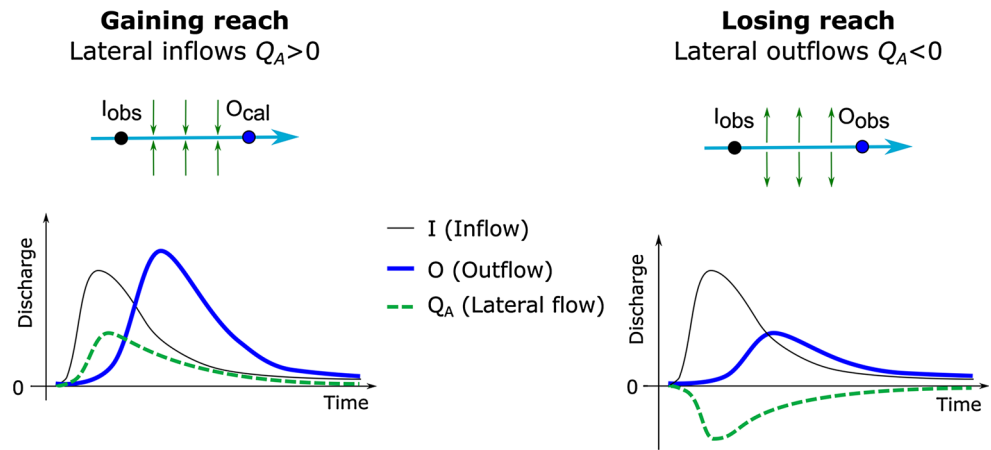


Fig. 4 Boxplots of total rainfall depth P per event (a) and maximum rainfall intensity measured over 1 h P_x (b) for the hydro-geomorphological hard-rock and karst areas during 30 storm events

mountainous part of the basin, this result highlights the strong orogenic effect on their rainfalls. Consequently, the highest runoff production from these head-basins should be taken into account when analysing flood propagation through the karstic areas in the Causses.

Losing and gaining reaches

Analysis of the spatial variability of lateral flow depths indicates the lateral inflows (gaining reaches) and lateral outflows (losing reaches) during a flood event. Figure 5 plots the lateral flow depth as a function of rainfall depth for all 30 flood events, with positive and negative lateral flow depth values indicating inflows and outflows, respectively. This representation shows the spatial distribution of the hydrological response during a flood,

highlighting the losing and/or gaining reaches. For example, the lateral flow depth distribution shows that Reach 1 can be either a losing or a gaining reach, whereas Reach 3 is a gaining reach only. On comparing Reaches 1, 2 and 3 in the Tarn River, the outflows seem to disappear downstream, with lateral inflow becoming the main process in the downstream area. Reach 4 in the Dourbie River has a similar pattern to Reach 2, with dominant lateral inflows but with losing occurrences in several flood events. The succession of attenuations or amplifications in the hydrological response from one reach to another one highlights the local influence of the various karstic aquifers along the river. To better understand this complex behaviour, the next section aims at quantifying the lateral flows on an hourly time step within a flood event.

Lateral flow modelling

To assess the dynamic of lateral flows along the hydrographic network, a modelling approach is used. First, an illustration of the methodology, based on a flood event, is presented to assess the ability of the modelling approach to simulate karstic lateral flows in a reach where lateral spring flows are measured (the 02 Nov. 2008 flood event in “[Illustration of the forward and inverse modelling approaches](#)”). Then, this approach is applied to two other events with spatially homogeneous and spatially contrasted distributed rainfalls, respectively (i.e. the 10 Apr. 2009 and 20 Oct. 2006 flood events in “[Spatio-temporal variability of lateral flows](#)”).

Illustration of the forward and inverse modelling approaches

The 02 Nov. 2008 flood event on Reach 4, between the Nant and Massebiau stations of the Dourbie River, has been selected (Fig. 6) to illustrate the DW model functioning using both the forward and inverse approaches. The

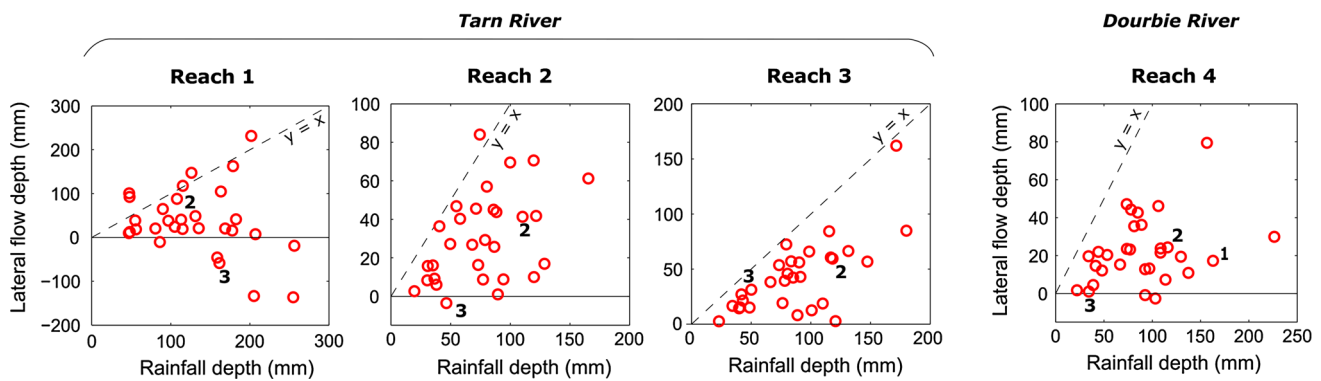
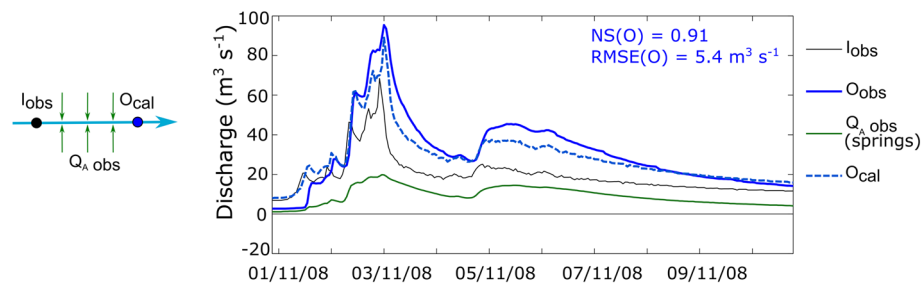


Fig. 5 Lateral flow depth vs. rainfall depth for 30 flood events in the four reaches of the Tarn and Dourbie rivers (see Fig. 2 for reach locations); positive and negative values of lateral flow depth indicate inflows and outflows, respectively; labels refer to the following

events: the 02 Nov. 2008 flood presented in Fig. 6 (Label 1), and the 10 Apr. 2009 (Label 2) and 20 Oct. 2006 (Label 3) floods presented in Fig. 7

(a) Forward model

Calculating the outflow $O(t)$ knowing the inflow $I(t)$ and the lateral flow $Q_A(t)$



(b) Inverse model

Calculating the lateral flow $Q_A(t)$ knowing the inflow $I(t)$ and the outflow $O(t)$

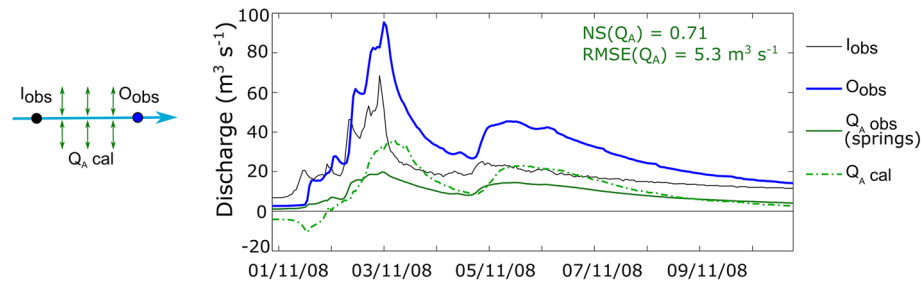


Fig. 6 Forward (a) and inverse (b) approaches of the DW model for the 02 Nov. 2008 flood event in the Dourbie River between the Nant (Inflow) and Massebiau (Outflow) stations (Reach 4); Obs and Cal refer to observed and calculated values, respectively; NS and RMSE are the Nash and Sutcliffe coefficient and the root mean square error, respectively

main obvious karst inflows on this reach are monitored at the Espérelle and Durzon springs.

Figure 6a presents the forward model simulation of the outflow hydrograph (dashed blue line) from the observed inflow hydrograph (solid black line) and observed lateral flow (solid green line) corresponding to the sum of the Espérelle and Durzon spring hydrographs. The performance criteria (Nash and Sutcliffe coefficient NS and the root mean square error RMSE) give good results for the outflow simulation [$NS(O) = 0.9$ and $RMSE(O) = 5.4 \text{ m}^3$

s^{-1}], indicating that the observed spring flows explain most of the lateral flows for this event in the reach.

Figure 6b presents the inverse model simulation of the lateral flow hydrograph (dash-dot green line) from the observed inflow hydrograph (solid black line) and the observed outflow hydrograph (solid blue line). The acceptable performance criteria [$NS(Q_A) = 0.7$ and $RMSE(Q_A) = 5.3 \text{ m}^3 \text{ s}^{-1}$] show the ability of the DW model to determine the dynamic of the lateral flows between two gauging stations.

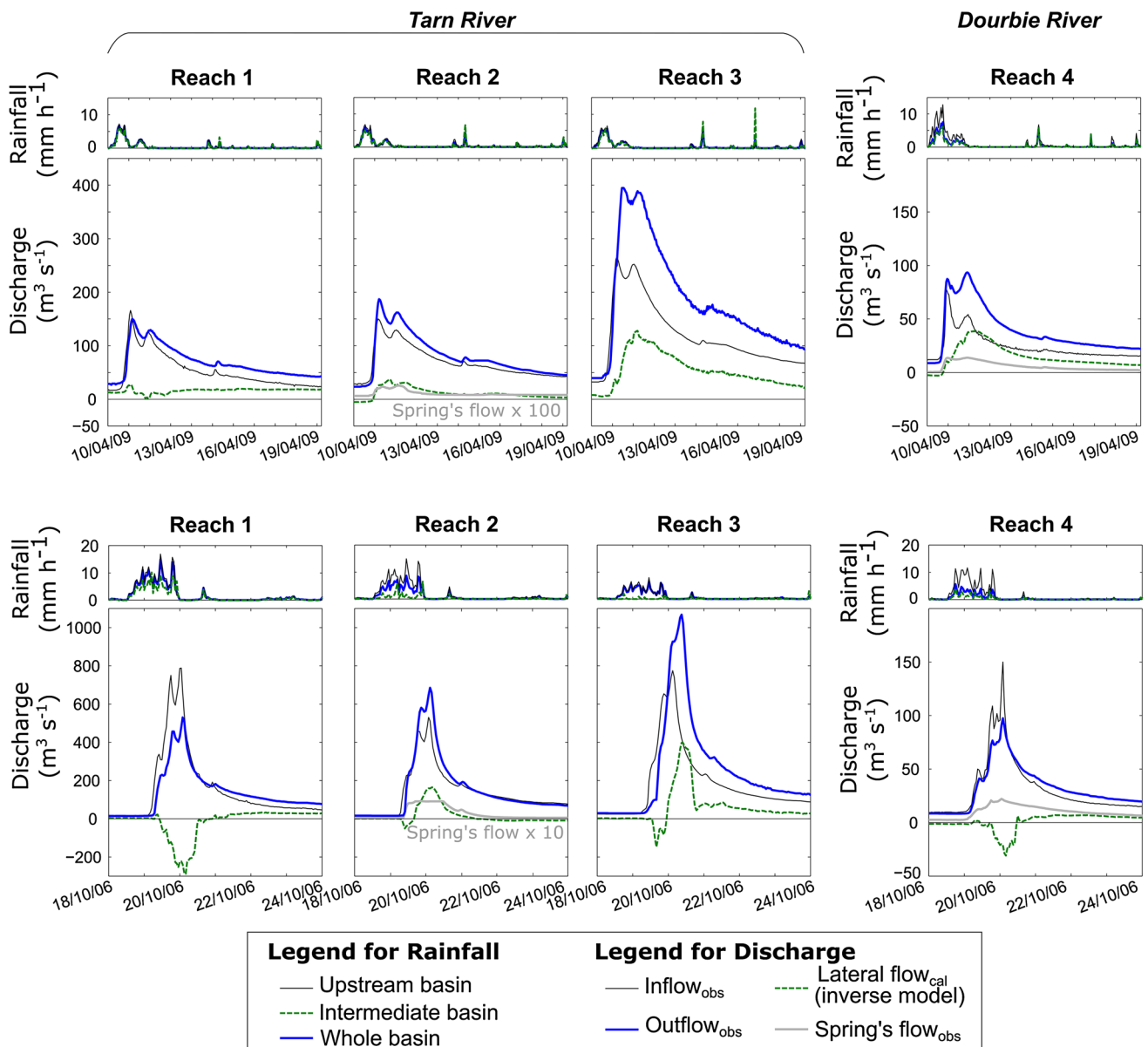


Fig. 7 Simulated lateral hydrographs of the Tarn and Dourbie river sub-basins for the 10 Apr. 2009 (*top*) and 20 Oct. 2006 (*bottom*) flood events; locations and characteristics of the sub-basins are given in Fig. 2 and Table 1, respectively

Regarding simulations obtained using the inverse model, the calculated lateral flow hydrograph is well simulated for periods of recession, but overestimated for periods of peakflow. It is interesting to note a decrease of the baseflow by about $8 \text{ m}^3 \text{ s}^{-1}$ in the channel between the two stations at the beginning of the flood, even though the springs were flowing at a rate of $5 \text{ m}^3 \text{ s}^{-1}$. This shows the complexity of lateral contributions in a channel reach where lateral inflows (localised springs) and outflows (river losses) occur concomitantly along the reach. The modelling approach is able to calculate the global lateral hydrograph, which is the sum of all the lateral inflows and outflows. This analysis also justifies the use of a model that accounts for

uniformly—rather than concentrated—distributed lateral flows when concentrated inflows (springs) and outflows (river losses) are not known and thus not precisely localised.

Spatio-temporal variability of lateral flows

To assess the effect of the spatial distribution of rainfall on the hydrological response, especially between the head-basin in the hard-rock area and the downstream karstic area, two events have been selected with similar river and spring baseflow levels indicating comparable initial hydrological and karst storage conditions, respectively.

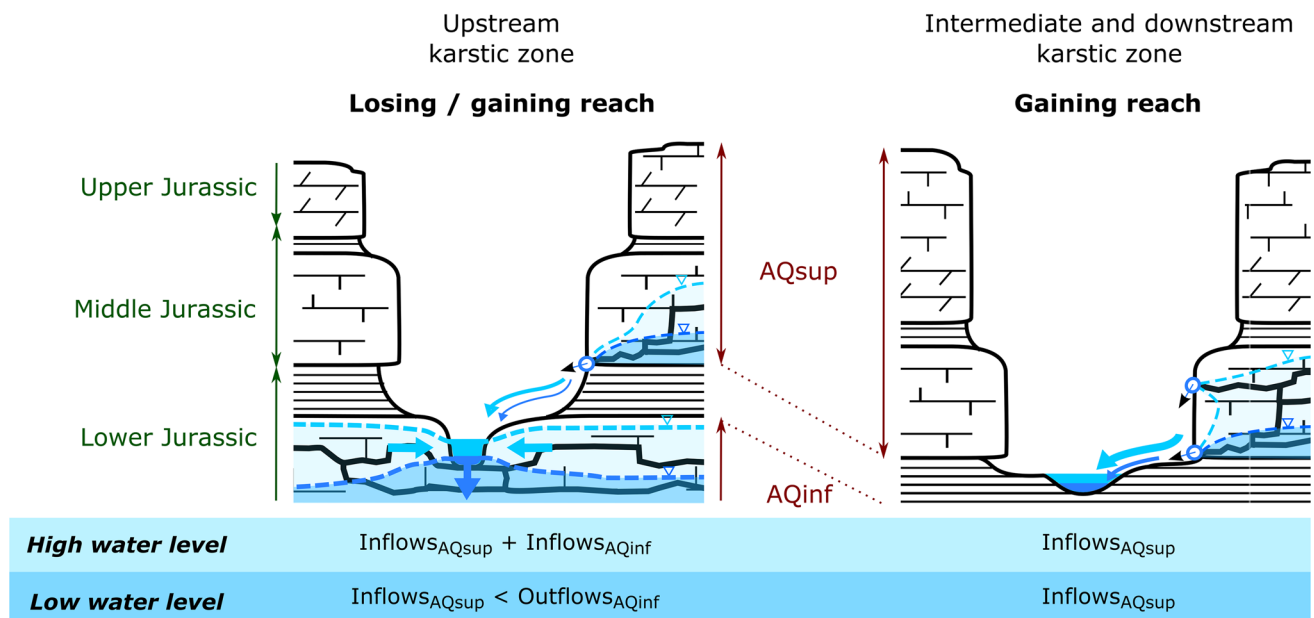


Fig. 8 Conceptual hydro(geo)logical model of the main karstic rivers in the Grands Causses area showing the role of the two overlapping aquifers (AQ) on the hydro(geo)logical response variability between the upstream and downstream karstic zones

The first flood event (10 Apr 2009) occurred under a spatially homogeneous rainfall distribution, while the second one (20 Oct 2006) occurred under a spatially contrasted rainfall distribution with up to four times higher rainfall intensities and amounts in the hard-rock area (head-basin).

Figure 7 presents the measured inflow and outflow, and calculated lateral flow hydrographs for each reach using the inverse model. First, with the homogeneous spatial rainfall distribution (top of Fig. 7), lateral inflow is observed for all the reaches, with an increase in lateral flow peaks from the upstream Reach 1 to the downstream Reach 3. In Reach 2, the calculated lateral hydrograph fits the measured spring's hydrograph multiplied by 100. The same pattern is also observed in Reach 4 on the Dourbie River, indicating that karst aquifers may explain the global lateral flow dynamic in the intermediate and downstream parts of the basin.

Second, with the contrasted spatial rainfall distribution (bottom of Fig. 7), a varied hydro(geo)logical response is observed in the reaches. High lateral outflows are estimated in the intermediate part of the basin for the two Reaches 1 and 4 located downstream of the head-basins at the hard-rock/karst boundary (cf. Figure 2); up to $280 \text{ m}^3 \text{ s}^{-1}$ of instantaneous outflows are estimated for Reach 1. Downstream, the model simulated both losses and gains during the flood, indicating that the flood wave is partly (25 % of the flood peak) re-infiltrated through the river bed once the stream reaches the karstic area.

Discussion and conclusion

The aim of this paper has been to characterise lateral flow variability in the Tarn River during flood events to improve the knowledge of the conceptual hydrogeological model of the Grands Causses massif drained by the river. Since lateral contributions to the river are controlled mostly by karst aquifers, the hydrological response is used as an indicator of the hydrogeological functioning.

The results have shown that with the DW model, which is simple, parsimonious and easy-to-use, it is possible to quantify lateral flows in heterogeneous media, such as karstic basins where complex surface/groundwater exchanges occur with high inflows from large springs as well as high river losses. The inverse model was used to assess the lateral contributions from karst systems along a channel reach; it simulates the uniformly distributed lateral hydrograph from observed input and output hydrographs. Previous work has shown the ability of time series analysis (Bailly-Comte et al. 2008b) and the kinematic wave model coupled with a linear reservoir of lateral inflows (Bailly-Comte et al. 2012) to assess surface/groundwater exchanges in karstic basins. Here, however, this paper presents the first physically based modelling approach that enables simulations for both distributed lateral inflows and outflows. This makes it possible, within a flood event, to quantify the temporal variability of lateral flows $Q_A(t)$ where river losses and gains and karstic spring inflows occur. Advantages of the DW model are a parsimonious parameterization using only two parameters

(celerity C and diffusivity D). The Hayami model also offers an unconditionally stable method, unlike numerical methods which induce numerical instabilities (Moussa and Bocquillon 1996a, b). Finally, the short time step analysis of the results has shown that the modelling approach may be used as a diagnostic tool to investigate, with more precision, the dynamics of lateral flows from an analysis of flood characteristics (e.g. lag time, rising limb, peakflow, recession curve). For example, Fig. 6b shows that the inverse model simulated a delayed lateral flow peak; this may indicate that some concentrated inflows are not well captured, meaning that the processes involved in lateral flow are not only diffusive. This type of analysis needs to be completed by a parameter uncertainty analysis on a large number of flood events.

Application of the DW model to the Tarn River (Southern France) has provided insights for the conceptual hydro(geo)logical model of the large Grands Causses area. First, analysis of the evolution of the lateral flow depths along the stream shows that the hydrological response from the head-water catchments is greatly modified where the river crosses the karstic area. Whereas large flows are generated by high rainfalls in the hard-rock area of the Cévennes mountains, the reaches at the hard-rock/karst boundary can show alternatively losses and gains. With the large number of gauging stations enabling the basin to be subdivided into sub-basins to limit the lateral inflows from tributaries, we have been able to ascertain that the changes in hydrological response along the river in the karstic area appear to be linked to the lateral surface/groundwater exchanges. Thus, as observed by previous authors (Bailly-Comte et al. 2008a; Zanon et al. 2010), the karstic terrain provides a major control on the flood response in regions impacted by a storm. De Waele et al. (2010) already determined that, depending on the reach's location on the river profile, this results in water losses and/or gains due to the high spatial variability of the hydrogeological karst features. The simulations also show that in places the lateral flow direction can change from outflow to inflow during a flood. According to the work of Bailly-Comte et al. (2009) in a Mediterranean karstic area, river losses may occur when the groundwater level is low. In the case study, however, this appears more complex because the analysis in the Dourbie River reach (Reach 4) shows that river losses occur even with large spring flows feeding the stream at the same time. This implies the presence of two superposed aquifers with various saturation levels relative to the altitude of the river bed. A diagram (Fig. 8) illustrating the conceptual model of karstic contributions to the Tarn River and its tributaries shows (1) a lower aquifer for which the main outlet is the stream via multiple springs localised in the river bed, and (2) an upper aquifer for which the outlets of the different units are localised at the bottom of the cliffs above the river bed. According to the classical hydrogeological

pattern of the Grands Causses area, the lower aquifer is developed in the Lower Jurassic exposed in the upstream karstic zones, whereas the upper aquifer is developed in the Middle and Upper Jurassic overlying Toarcian marl in the downstream zones.

A last point is that these results help us to better understand flood generation in Mediterranean karstic areas where the head-water basins—commonly located in hard-rock areas such as the Cévennes or Pyrenees—have the highest rainfall intensities. Results show that the role of surface/groundwater exchange varies greatly with distance from the hard-rock/karst boundary (i.e. where allogenic recharge from the hard-rock area occurs). With a homogeneous rainfall distribution over the area, stream losses are not visible, even at the hard-rock/karst boundary, and the flood is amplified all along the channel reach towards the outlet. With a contrasted rainfall distribution over the area (up to four times higher rainfall intensities in the head-water basin compared to the karst area), the upstream reaches of the karst area have a dominant peakflow attenuation role by re-infiltrating part of the runoff, whereas the downstream reaches of the karst area have a dominant amplification role: small stream losses occurring at the beginning of the flood are followed, during peakflow, by high inflows from karst units. These results give a better understanding of flood generation in such contexts where Delrieu et al. (2005) observed lower runoff coefficient values for the karstic catchment compared to the hard-rock catchment in the eastern zone of the Cévennes mountains. Finally, this study revealed highly variable flood peak attenuation or amplification from karst units along the stream channel during a single flood event, which makes it more difficult to forecast the karst influence on flood generation. The new methodology proposed here opens challenging perspectives towards a framework for the analysis of short time step lateral inflows/outflows in rivers leading to a better understanding surface–groundwater exchanges in karstic zones.

Acknowledgments This work was funded by the French Governmental Administration for Risk Prevention (*DGPR*), the *Service Central d'Hydrométéorologie et d'Appui à la Prévision des Inondations (SCHAPI)*, and the French Geological Survey (*BRGM*). The authors thank Laurent Voronovas and Didier Fabre from the Flooding Forecast Office (*Service de Prévision des Crues Garonne-Tarn-Lot*) for providing hydrological data. They also thank the two reviewers and editors for their constructive comments that help improve the manuscript.

References

- ADES (2012) portail ADES. <http://www.ades.eaufrance.fr/> (data exported in July 2012)
- Ambert P, Martin PH, Guendon J-L (1994) Le canyon de la Dourbie et le karst de la source de l'Espérelle. *Etudes de Géographie Physique*, XXIII: 63–80
- Bailly-Comte V, Jourde H, Roesch A, Pistre S (2008a) Mediterranean flash flood transfer through karstic area. *Environ Geol* 54(3):605–614. doi:10.1007/s00254-007-0855-y

- Bailly-Comte V, Jourde H, Roesch A, Pistre S, Batiot-Guilhe C (2008b) Time series analyses for karst/river interactions assessment: case of the Coulazou River (southern France). *J Hydrol* 349(1–2):98–114. doi:10.1016/j.jhydrol.2007.10.028
- Bailly-Comte V, Jourde H, Pistre S (2009) Conceptualization and classification of groundwater-surface water hydrodynamic interactions in karst watersheds: case of the karst watershed of the Coulazou River (southern France). *J Hydrol* 376(3–4):456–462. doi:10.1016/j.jhydrol.07.053
- Bailly-Comte V, Borrell-Estupina V, Jourde H, Pistre S (2012) A conceptual semidistributed model of the Coulazou River as a tool for assessing surface water–karst groundwater interactions during flood in Mediterranean ephemeral rivers. *Water Resour Res* 48:W09534. doi:10.1029/2010wr010072
- Bérard P (1987) Protection des captages AEP situés en terrains calcaires—Cause Majeurs de la Lozère. BRGM report 87-SGN-163-LRO, p 79
- Bonacci O, Ljubenkov I, Roje-Bonacci T (2006) Karst flash floods: an example from the Dinaric karst (Croatia). *Nat Hazards Earth Syst Sci* 6:195–203. doi:10.5194/nhess-6-195-2006
- Braneyre M, Malatrait A, Durand V, Violet J, Brunet M (1999) Etude hydrogéologique du Causse Rouge (Aveyron)—Connaissance, aménagement et protection des ressources en eau souterraine. ANTEA report A 12245:150
- Charlier J-B, Bailly-Comte V, Desprats J-F (2012) Appui au SCHAPI 2012—Module 1—Mise en place d'un indicateur d'aide à la décision pour la prévision de crue en milieu karstique : le bassin du Tarn à Millau. BRGM report RP-61816-FR, p 88
- Cimorelli L, Cozzolino L, Della Morte R, Pianese D (2014) Analytical solutions of the linearized parabolic wave accounting for downstream boundary condition and uniform lateral inflows. *Adv Water Resour* 63:57–76. doi:10.1016/j.advwatres.2013.11.003
- De Waele J, Martina MLV, Sanna L, Cabras S, Cossu QA (2010) Flash flood hydrology in karstic terrain: flumineddu Canyon, central-east Sardinia. *Geomorphology* 120(3–4):162–173. doi:10.1016/j.geomorph.2010.03.021
- Delrieu G, Ducrocq V, Gaume E, Nicol J, Payrastra O, Yates E, Kirstetter PE, Andrieu H, Ayrat PA, Bouvier C, Creutin JD, Livet M, Anquetin S, Lang M, Neppel L, Oblé C, Parent-du-Chatelet J, Saulnier GM, Walpersdorf A, Wobrock W (2005) The catastrophic flash-flood event of 8–9 September 2002 in the Gard Region, France: a First Case Study for the Cévennes-Vivarais Mediterranean Hydrometeorological Observatory. *J Hydrometeorol* 6:34–52. doi:10.1175/JHM-400.1
- Dörflinger N (2007) Etude hydrogéologique du Causse de Sauveterre et de ses avants-causses (secteur Est), Lot No 5: Synthèse, BRGM report BRGM/RP-55529-FR, p 95
- Dörflinger N, Meus PH (2006) Etude hydrogéologique du Causse de Sauveterre et de ses avants-causses (Secteur Est), Lot no 4: Traçages, BRGM report BRGM/RP-55160-FR, p 237
- Fleury P, Maréchal JC, Ladouche B (2013) Karst flash-flood forecasting in the city of Nîmes (southern France). *Eng Geol* 164:26–35. doi:10.1016/j.enggeo.2013.06.007
- Hayami S (1951) On the propagation of flood waves. *Disaster Prev Res Inst Bull* 1:1–16
- Jourde H, Roesch A, Guinot V, Bailly-Comte V (2007) Dynamics and contribution of karst groundwater to surface flow during Mediterranean flood. *Environ Geol* 51(5):725–730. doi:10.1007/s00254-006-0386-y
- Jourde H, Lafare A, Mazzilli N, Belaud G, Neppel L, Doerflinger N, Cernesson F (2013) Flash flood mitigation as a positive consequence of anthropogenic forcings on the groundwater resource in a karst catchment. *Environ Earth Sci* 71:573–583. doi:10.1007/s12665-013-2678-3
- Kourgialas NN, Karatzas GP, Nikolaidis NP (2012) Development of a thresholds approach for real-time flash flood prediction in complex geomorphological river basins. *Hydrol Process* 26:1478–1494. doi:10.1002/hyp.8272
- Lecollinet P (2012) Courbe de tarage de la station de Florac Bécède sur le Tarnon. SPC Tarn-Lot, Report, p 20
- Lopez-Chicano M, Calvache ML, Martin-Rosales W, Gisbert J (2002) Conditioning factors in flooding of karstic poljes—the case of the Zafarraya polje (South Spain). *CATENA* 49(4):331–352
- Marchandise A (2007) Modélisation hydrologique distribuée sur le Gardon d'Anduze; étude comparative de différents modèles pluie-débit, extrapolation de la normale à l'extrême et tests d'hypothèses sur les processus hydrologiques, PhD thesis, Univ. Montpellier 2, p 214
- Maréchal JC, Ladouche B, Dörflinger N (2008) Karst flash flooding in a Mediterranean karst, the example of Fontaine de Nîmes. *Eng Geol* 99(3–4):138–146. doi:10.1016/j.enggeo.2007.11.013
- Mijatovic B (1988) Catastrophic flood in the polje of Cetinje in February 1986, a typical example of the environmental impact of Karst. *Environ Geol* 12(2):117–121
- Moussa R (1996) Analytical Hayami solution for the diffusive wave flood routing problem with lateral inflow. *Hydrol Process* 10(9):1209–1227
- Moussa R, Bocquillon C (1996a) Algorithms for solving the diffusive wave flood routing equation. *Hydrol Process* 10(1):105–124
- Moussa R, Bocquillon C (1996b) Criteria for the choice of flood-routing methods in natural channels. *J Hydrol* 186(1–4):1–30
- Moussa R, Bocquillon C (2009) On the use of the diffusive wave for modelling extreme flood events with overbank flow in the flood-plain. *J Hydrol* 374:116–135. doi:10.1016/j.jhydrol.2009.06.006
- Moussa R, Voltz M, Andrieux P (2002) Effects of the spatial organization of agricultural management on the hydrological behaviour of a farmed catchment during flood events. *Hydrol Process* 16:393–412. doi:10.1002/hyp.333
- Moussa R, Chahinian N, Bocquillon C (2007) Distributed hydrological modelling of a Mediterranean mountainous catchment—model construction and multi-site validation. *J Hydrol* 337:35–51. doi:10.1016/j.jhydrol.2007.01.028
- PNRGC, Cadier S (2010) Etude hydrogéologique du Causse Noir, cahier des clauses techniques particulières Version 1, Parc Naturel Régional des Grands Causses report, p 29
- Pinault J-L, Plagnes V, Aquilina L, Bakalowicz M (2001) Inverse modeling of the hydrological and the hydrochemical behavior of hydrosystems; characterization of karst system functioning. *Water Resour Res* 37(8):2191–2204
- Plagnes V (1997) Structure et fonctionnement des aquifères karstiques. Caractérisation par la géochimie des eaux. Ph.D. thesis, Univ. Montpellier 2, p 376
- PNRGC (2006) Etude hydrogéologique de la partie ouest du Causse de Sauveterre et de ses avants Causses. Parc Naturel Régional des Grands Causses report, p 279
- PNRGC (2011) Gestion du risque pour la santé publique : réalisation de traçages en aval des bassins de décantation situés sur des périmètres de protection de sources captées pour l'alimentation en eau potable—Cause du Larzac (bassins du Durzon, de l'Espérelle et de l'Homède). Parc Naturel Régional des Grands Causses report, p 21
- Ricard J, Bakalowicz M (1996) Connaissance, aménagement et protection des ressources en eau du Larzac septentrional, Aveyron (France), BRGM report R38953, p 94
- Zanon F, Borga M, Zoccatelli D, Marchi L, Gaume E, Bonnifait L, Delrieu G (2010) Hydrological analysis of a flash flood across a climatic and geologic gradient: the September 18, 2007 event in Western Slovenia. *J Hydrol* 394:182–197. doi:10.1016/j.jhydrol.2010.08.020